Title

A field-modeling study for assessing temporal variations of soil-water-crop interactions under water-saving irrigation strategies

Journal

Agricultural Water Management, 178(C)

ISSN

0378-3774

Authors

Karandish, Fatemeh
Šimůnek, Jiří

Publication Date

2016-12-01

DOI

10.1016/j.agwat.2016.10.009

Peer reviewed

Agricultural Water Management 178 (2016) 291–303

Contents lists available at ScienceDirect

Agricultural Water Management

journal homepage: www.elsevier.com/locate/agwat

A field-modeling study for assessing temporal variations of soil-water-crop interactions under water-saving irrigation strategies

Fatemeh Karandish[a,*], Jiří Šimůnek[b]

[a] Water Engineering Department, University of Zabol, Zabol, Iran
[b] Department of Environmental Sciences, University of California Riverside, Riverside, CA 92521, USA

ARTICLE INFO

Article history:
Received 3 May 2016
Received in revised form
27 September 2016
Accepted 9 October 2016

Keywords:
HYDRUS-2D
Maize grain yield
Partial root-zone drying
Soil water balance components
Water repartition

ABSTRACT

Simulation models are useful tools that may help to improve our understanding of soil-water-plant interactions under innovative water-saving irrigation strategies. In this study, the HYDRUS-2D model was applied to evaluate the influence of deficit irrigation (DI) and partial root-zone drying (PRD) on maize water extractions during two cropping cycles of 2010 and 2011. The model was calibrated and validated using measured soil water content data (expressed as equivalent water depths). Reliable estimates of soil water content were provided by HYDRUS-2D, with root mean square error and mean bias error values of 2.3–5.11 and 1.63–4.93 mm, respectively. Root water uptake and maize grain yields were reduced by 13.2–28.8% and 13.6–52.8%, respectively, under different water-saving irrigation treatments compared to full irrigation. However, different root and water repartitions in the PRD treatment with a 25% reduction in the irrigation depth (PRD_{75}) improved soil water utilization and consequently, crop growth. Increased root water uptake (2.2–4.4 times higher than in other treatments) from the 60–100 cm soil depth in the PRD_{75} treatment maintained a favorable daily evapotranspiration rate, resulting in no significant reduction in maize grain yield compared to full irrigation. Consequently, a 15.7–85% increase in water use efficiency for maize cultivation under PRD_{75} ensured 25% water savings without threatening food security in the study area. It can be concluded that HYDRUS-2D can be successfully used to optimize water management under local water-stress conditions.

1. Introduction

The reduction in fresh water resources due to climate change and rapid growth of the world's population often leads to severe competition between industrial, municipal, and environmental users of water (Alberto et al., 2014). Agriculture is the biggest fresh water user all over the world and commands over 70% of the world's freshwater withdrawals (OECD, 2010). Indeed, to feed the growing worldwide population and banish hunger from the world, food and animal feed production will need to be significantly increased (Darzi-Naftchali and Shahnazari, 2014), requiring the allocation of even more fresh water to agriculture. Consequently, irrigated agriculture has been widely developed over the past few decades. Nevertheless, since sustainable agriculture needs to be achieved with limited fresh water resources, exposing plants to water stress will become unavoidable.

Under such circumstances, deficit irrigation (DI) has been developed as a water-saving irrigation strategy where crops receive less irrigation water during their growing season. However, although adapting DI may be a rational decision under an existing water crisis (Karandish et al., 2015), it may lead to a significant yield loss (Payero et al., 2006) that may threaten food security. Therefore, it is essential to find an efficient water saving method to sustain local social and economic developments. During recent decades, an efficient irrigation method named partial root-zone drying (PRD) has been developed (Dry and Loveys, 1998). In this method, one half of the root zone is irrigated while the other half is allowed to dry out. The irrigated and dry sides are periodically switched. It has been reported that this water-saving irrigation method can reduce irrigation amounts without reducing crop yield and hence can increase water and nutrient use efficiencies (Kang and Zhang, 2004; Shao et al., 2008; Karandish and Shahnazari, In press).

Nevertheless, some researchers have demonstrated that reducing the amount of irrigation water under PRD should be done with special caution because the resulting water stress may affect crop

* Corresponding author at: Water Engineering Department, Water and Soil Faculty, University of Zabol, Zabol, Iran.
E-mail addresses: F.Karandish@uoz.ac.ir, Karandish_h@yahoo.com (F. Karandish).

http://dx.doi.org/10.1016/j.agwat.2016.10.009
0378-3774/

yields if it is higher than the plants' tolerance. Liu et al. (2006) reported that although a 25% reduction in irrigation water during a potato growth season significantly increased the irrigation water use efficiency (IWUE), a further 45% reduction led to a significant decrease in yield and IWUE. Similar results were reported by Karandish and Shahnazari (In press) for maize. These results could be associated with a linear relationship between root water uptake and yield under water stress conditions (Traore et al., 2000). Many researchers reported that the effects of water stress on yield depend on how significantly the stress affects the crop evapotranspiration (Payero et al., 2006; Klocke et al., 2004; Stone, 2003). Therefore, a better understanding of daily soil-water-plant interactions may help to improve the water use efficiency under water-saving irrigation strategies, since such knowledge may lead to finding optimal levels of the water stress, preventing significant yield losses and producing optimal irrigation scheduling.

These goals could be achieved using laborious and time-consuming, and therefore expensive, field investigations. As a result, direct measurements of soil water dynamics and soil-water-plant interactions under PRD have rarely been carried out. Previous research has focused mainly on PRD effects on yield and crop physiological responses (Kang and Zhang, 2004; Shao et al., 2008; Karandish and Shahnazari, In press). Modeling could be an alternative tool to identify optimal conditions for applying PRD, especially when the project is economically or technically impossible to be carried out in the field (Li and Liu, 2011).

Among the different available models, HYDRUS-2D (Šimůnek et al., 2008, 2016) has been extensively and successfully used to simulate daily soil water dynamics under many different conditions (e.g., Cote et al., 2003; Gärdenäs et al., 2005; Ajdary et al., 2007; Doltra and Munoz, 2010). However, a review of the literature indicates that no research has been done on evaluating HYDRUS-2D for PRD conditions, especially for PRD involving surface drip irrigation (SDI). Meanwhile, SDI is becoming a widely accepted irrigation method that minimizes leaching and improves water and fertilizer use efficiencies due to its advantage of applying water in precise amounts and at exact locations throughout the field (Bar-Yosef and Sheikholslami, 1976).

PRD-SDI is expected to be an efficient irrigation strategy for many crops because it has both the advantages of PRD and SDI. However, there is a lack of knowledge about soil-water-plant interactions under PRD-SDI and therefore a need to identify the optimal management for this irrigation strategy. To address this issue, a two-year field investigation was carried out in a maize field equipped with an SDI system under full irrigation and both DI-SDI and PRD-SDI strategies to evaluate the following objectives: (i) to calibrate and validate HYDRUS-2D for simulating various soil water balance components; (ii) to describe daily variations of soil water balance components; and (iii) to compare soil-water-plant interactions and evaluate the most water efficient irrigation strategy within the study area.

2. Materials and methods

2.1. Field trial

A two-year field investigation was carried out in a 15 × 55 m maize field at the Sari Agricultural Sciences and Natural Resources University (SANRU: 36.3°N, 53.04°E; 15 m below sea level). Climatic variables during the study period (i.e., maize growing seasons of 2010 and 2011) are displayed in Fig. 1, which shows daily recorded weather data collected at the weather station near the experimental field. Daily mean air temperatures (T) in 2010 were between 0.1 and 7.8 °C higher than in 2011. Both vapor pressure deficits (VPD) and net radiations (R_n) followed the same seasonal trend as temperatures. During more than 66% of days in 2010, R_n was between about 0.3 and 56.8% higher than in 2011. Total precipitations of 8 and 40 mm were recorded during the entire growing seasons of 2010 and 2011, respectively. There was no rainfall 55 and 45 days after planting (DAP) in 2010 and 2011, respectively. Selected soil physical properties for the study area are summarized in Table 1.

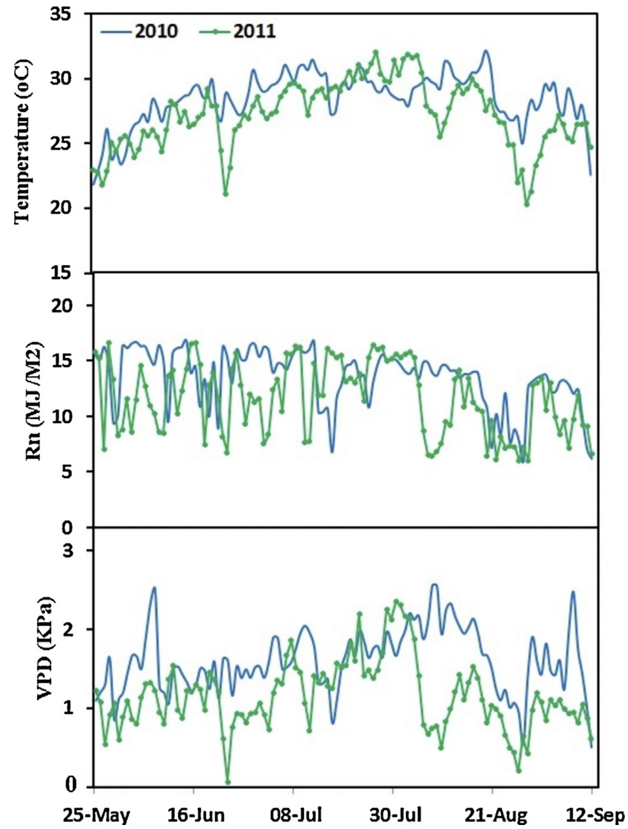

Fig. 1. Daily mean temperatures (a), net radiations (R_n) (b), and vapor pressure deficits (VPD) (c). during two growing seasons of 2010 and 2011.

A complete block design with five SDI treatments [full irrigation (FI), two partial root-zone drying (PRD) treatments (PRD_{75} and PRD_{55}), and two deficit irrigation (DI) treatments (DI_{75} and DI_{55})] in three replicates was used in the field trial. The surface drip irrigation system was installed before sowing. Drip lines with emitters 20 cm apart and an emitter discharge rate of 2 L h^{-1} were placed on the soil surface 75 cm apart (Fig. 2a).

Thereafter, for each treatment, five 100 cm long TDR probes (Trime FM; IMKO; Germany) were installed as illustrated in Fig. 2b (i.e., 25 TDR probes were installed in the study area; 5 probes × 5 treatments). TDR probes were used at least two times a day to measure soil water contents (SWCs) at depths of every 5 cm (i.e., at measuring points displayed in Fig. 2b) during both growing seasons. Overall, SWCs were measured at each measuring time in 100 points for each treatment. Moreover, information about the movement of the wetting front during irrigation events was collected at least 10 times in each treatment by measuring SWCs one hour before, and immediately and 2, 6, 12, 24, 48, 72, and 96 h after the irrigation events in the 2010 growing season. To measure retention curves, soil samples were taken every 20 cm to a depth of 80 cm for each treatment in three replicates. SWCs at 11 different pressure heads were measured in the laboratory at each sample using a pressure plate apparatus.

The single-cross, hybrid maize 704 was then planted 5 cm deep; parallel to and between the drip lines on May 26 (in both 2010 and 2011), at 75 × 20 cm row and crop spacings (Fig. 2a). The experi-

Table 1
Soil physical properties in the study area.

Depth (cm)	Soil texture	Field capacity (%)	Wilting point (%)	Bulk density ($g\,cm^{-3}$)
0–20	Sandy clay loam	30	15	1.4
20–40	Clay loam	32	14	1.38
40–60	Clay loam	32	14	1.35
60–80	Clay loam	32	14	1.37
80–100	Clay loam	32	14	1.37

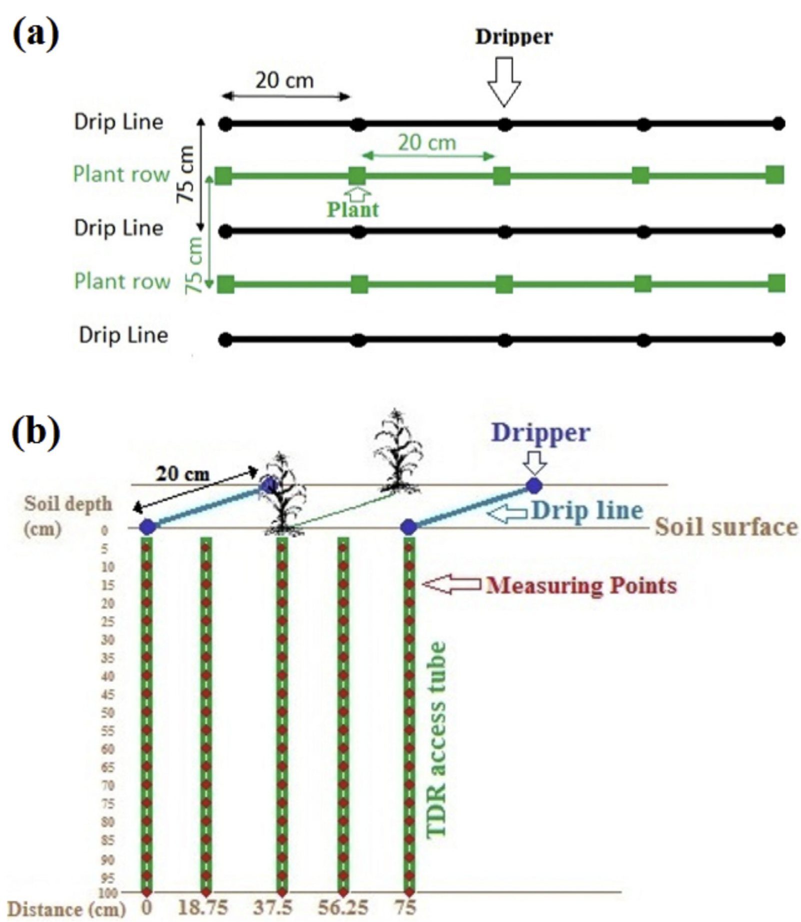

Fig. 2. Schematic of the field experimental site. Horizontal locations of laterals, drippers, and plants in the experimental field (a) and locations of TDR probes in the maize root zone (b).

mental plots were irrigated every other day during both growing seasons. For the FI treatment, the net irrigation depth ($[I_n]_{FI}$, mm) was calculated as follows:

$$[I_n]_{FI} = \sum_{i=1}^{j} ((\theta_{FCi} - (\theta_{BIi})_{FI}) \times D_i) \quad (1)$$

where θ_{FCi} is the volumetric soil water content at field capacity ($cm^3\,cm^{-3}$) of the ith soil layer (field capacity for individual soil layers was determined prior to the field experiment), $(\theta_{BIi})_{FI}$ is the volumetric soil water content before irrigation in the ith soil layer ($cm^3\,cm^{-3}$) in the FI treatment, D_i is the soil layer thickness (mm), i is the soil layer counter, and j refers to the number of soil layers for which $[I_n]_{FI}$ is calculated. $(\theta_{BIi})_{FI}$ is the average SWC measured using Time Domain Reflectometry (TDR) probes in different measuring points in the ith soil layer (Fig. 2). The net irrigation depth thus refers to the actual soil water depletion between two consecutive irrigation events under the FI treatment. Applying $[I_n]_{FI}$ will refill the pore space in the rooting zone to the field capacity.

All treatments received the same amount of irrigation water during the first 55 and 45 DAP in 2010 and 2011, respectively, which was prior to applying different irrigation treatments. Different irrigation treatments were not imposed during the early growth stage since it is commonly believed that initiating the PRD treatments in this stage may result in a significant reduction in crop's yield and crop's quality (e.g., Dry et al., 2000; Kang and Zhang 2004; Kirda et al., 2004; Tang et al., 2005; Shao et al., 2008). Similarly as done by others (e.g., Shahnazari et al., 2007; Yazar et al., 2009; Dry et al., 2000; Kang and Zhang, 2004; Kirda et al., 2004; Tang et al., 2005; Shao et al., 2008), applications of the PRD irrigation treatments were postponed until the midway of the corn growth season in order to sustain the positive effects of the PRD treatment on the water use efficiency. Different irrigation treatments were applied during 55–107 DAP in 2010 and 45–110 DAP in 2011. During this stress period, the PRD and DI treatments were scheduled to receive 55% (PRD_{55} and DI_{55}) or 75% (PRD_{75} and DI_{75}) of the calculated irrigation volume of the FI treatment (Eq. (1)) during each irrigation event. While in the DI treatments, the irrigation volume at each dripper was reduced by 25 or 45% (in DI_{75} and DI_{55}, respectively), in the PRD treatments one dripper line was alternatively not used at all, while the irrigation volume at the other dripper line was increased by 50 and 10% in PRD_{75} and PRD_{55}, respectively. Therefore, the vertical movement of irrigation water in the wetted side of the PRD treatments is expected to be more extensive than that for the DI or FI treatments. The irrigated and non-irrigated sides were switched weekly in the PRD treatments because the idea of using PRD as a tool to manipulate the plant water deficit response has its origin in the observation that root-generated Abscisic Acid (ABA) can be transported to shoot regulating stomata of the leaves. To sustain the effect of PRD on stomata, it is necessary to regularly alternate the wet and dry compartments, usually every 6–14 days (Shahnazari et al., 2007; Stoll et al., 2000; Yazar et al., 2009); the length of this period depends on crop species, evaporative demands, and soil conditions. Irrigated and non-irrigated sides of the PRD treatments were switched in this study weekly, as recommended for maize (Yazar et al., 2009).

During both growing seasons, plants were sampled in all treatments to determine temporal variations of the leaf area index and horizontal and vertical root distributions. *LAI* was determined at 55, 62, 69, 76, and 83 DAP in 2010 and at 40, 56, 63, 70, 77, and 90 DAP in 2011 for all treatments. At each sapling time, three plants per plot were harvested. A laboratory leaf area meter (Delta-t Devices Ltd.) was used to measure the entire leaf area, which was converted to *LAI* by dividing it with the corresponding soil surface covered by the plants. At the same time, the horizontal and vertical root distributions were determined using the Auger Sampling method (Kumar et al., 1993). Roots were sampled with a 2-in ID auger every 10 cm down to a depth of 80 cm and horizontally every 10 cm between two drip lines.

At the final harvest, the whole root system of one plant per each replicate of a treatment (i.e., three plants per treatments) was extracted and the root dry mass (*RDM*) was measured by oven drying roots at 70 °C for 24 h. Maize grain yields were also measured at the end of the cropping cycles. The plants were harvested on September 9, 2010 (107 DAP) and September 12, 2011 (110 DAP). The soil water contents (SWCs) collected during the FI and PRD treatments were used to assess the ability of various machine-learning techniques to predict SWCs in a study by Karandish and Šimůnek (in review).

2.2. Simulation approach

The HYDRUS (2D/3D) software (Šimůnek et al., 2008, 2016) simulates two- or three-dimensional variably-saturated water flow and root water uptake in soils. In this study, water movement was simulated in a two-dimensional vertical plane. The domain geometry was defined to represent a typical maize field in which driplines are located between maize rows with a row spacing of 75 cm (Fig. 2b). The domain geometry was defined to be 75 cm wide and 80 cm deep, with the driplines on the upper left and right corners of the domain and a maize plant in the middle of the domain surface. The 80 cm soil depth was selected so that the observed maximum rooting depth was situated above this depth. The driplines were considered to be line sources, since the emitter spacing along the driplines was relatively small (i.e., 20 cm in this field investigation) (Skaggs et al., 2004).

The following mixed form of the Richards equation, describing two-dimensional water flow in soil, was numerically solved using the finite element method (Šimůnek et al., 2011):

$$\frac{\partial\theta}{\partial t} = \frac{\partial}{\partial x}\left[K(h)\frac{\partial h}{\partial x}\right] + \frac{\partial}{\partial z}\left[K(h)\frac{\partial h}{\partial z}\right] + \frac{\partial K(h)}{\partial z} - S(x,z,h) \tag{2}$$

where x is the horizontal coordinate (L), z is the vertical coordinate taken as positive upward (L), t is the simulation time (T), θ is the volumetric soil water content (L^3L^{-3}), h is the soil water pressure head (L), $K(h)$ is the unsaturated hydraulic conductivity function (LT^{-1}), and $S(x,z,h)$ is root water uptake (T^{-1}). The equation of Feddes et al. (1978) was used for determining the root water uptake sink term of Eq. (2):

$$S(x,z,h) = \alpha(x,z,h)b(x_1,z_1)WT_p \tag{3}$$

where $\alpha(x,z,h)$ is the soil water stress response function (dimensionless), $b(x_1,z_1)$ is the normalized spatial root water uptake distribution (L^{-2}), W is the width of the soil surface associated with transpiration (L), and T_p is potential transpiration (LT^{-1}). Crop evapotranspiration (ET_c) under the FI treatment was supposed to represent the potential crop evapotranspiration (i.e., potential evapotranspiration of maize) since crops under the FI treatment were well-irrigated (i.e., there was no water stress in the rooting zone in the FI treatment since irrigation events in this treatment were always scheduled to refill soil water content to field capacity), well fertilized and were treated with pesticides to control weeds, aphids and fungal diseases during both growing seasons. Moreover, these crops achieved their full production when considering the maize yield potential for given climate conditions in the study area. ET_c in the FI treatment ($ET_{c\text{-FI}}$) was calculated using the soil water balance equation (Allen et al., 1998):

$$([I_n]_{\text{FI}} + P) + \Delta S_{RZ\text{-FI}} = DP_{RZ\text{-FI}} + ET_{c\text{-FI}} \times \Delta t \tag{4}$$

where $[I_n]_{\text{FI}}$ is the net irrigation water depth (mm) for the *FI* treatment, P is precipitation (mm), $\Delta S_{RZ\text{-FI}}$ is the change (depletion) in the soil water storage in the rooting zone between two irrigation events (mm), $DP_{RZ\text{-FI}}$ is the amount of deep percolation between two irrigation events (mm), $ET_{c\text{-FI}}$ is the crop evapotranspiration (mm/d), and Δt is the time interval between two irrigation events (d). $\Delta S_{RZ\text{-FI}}$ was calculated as the difference between the soil water storage at the beginning (S_1) and the end of a specific time period (S_2) (i.e., $\Delta S_{RZ} = S_1 - S_2$). $DP_{RZ\text{-FI}}$ was assumed to be zero since irrigation events in the FI treatment were scheduled to refill the pore space to field capacity in the rooting zone (Eq. (1)).

Measured leaf area index (*LAI*) was then applied to divide $ET_{c\text{-FI}}$ into potential evaporation (E_p) and potential transpiration (T_p) as follows (Belmans et al., 1983):

$$E_p = ET_c e^{-K_{gr}*LAI}$$
$$T_p = ET_c - E_p \tag{5}$$

where E_p is potential evaporation [LT^{-1}], T_p is potential transpiration [LT^{-1}], ET_c is crop evapotranspiration [LT^{-1}], and K_{gr} is an extension coefficient for global solar radiation [−]. K_{gr} was set to 0.39 following the suggestions by Ritchie (1972) and Feddes et al. (1978). Estimated values of E_p and T_p were used as input parameters in HYDRUS-2D.

The stress response function $\alpha(x,z,h)$ was obtained from the HYDRUS-2D database for maize (Šimůnek et al., 2011). The $b(x_1,z_1)$ function was defined according to Vrugt et al. (2001):

$$b(x_1,z_1) = \left[1 - \frac{x_1}{x_{1m}}\right]\left[1 - \frac{z_1}{z_{1m}}\right] e^{-(p_x/x_{1m})|x_1^* - x_1| + p_z/z_{1m}|z_1^* - z_1|} \tag{6}$$

where z_{1m} is the maximum rooting depth in the vertical direction, x_{1m} is the maximum rooting length in the horizontal direction, $x_1{}^*$ and $z_1{}^*$ are parameters that describe the location of maximum root water uptake in the horizontal and vertical directions, respectively, and p_x and p_z are the shape parameters for the horizontal and vertical directions, both set to 1 (Vrugt et al., 2001).

The van Genuchten-Mualem model (Mualem, 1976; van Genuchten, 1980) was used to describe the soil hydraulic properties. The soil hydraulic parameters for two soil horizons (i.e., 0–20 cm and 20–80 cm soil depths) were obtained by fitting this model to the observed retention curves data of both layers using the RETC software. Fitted soil hydraulic parameters included the saturated SWC (θ_s), the residual SWC (θ_r), and the shape parameters α and n. Since no hydraulic conductivity data was available, the pedotransfer functions embedded in the HYDRUS (2D/3D) software were used to predict the saturated soil hydraulic conductivity (K_s) using measured soil physical properties for each treatment.

Initial conditions were defined using the measured initial soil water contents of each soil layer. The time-variable flux and atmospheric boundary conditions were specified at the surface boundary. While a time-variable flux boundary condition was used to represent both emitters, an atmospheric boundary condition with specified values of precipitation, evaporation, and transpiration was used on the rest of the soil surface. A free drainage boundary condition was applied at the bottom boundary, allowing for downward drainage and leaching. All other remaining boundaries were assigned a zero water flux boundary condition.

Calibration and validation are two important processes that ensure the optimal use of a model. Therefore, HYDRUS-2D should first be calibrated and validated to correctly simulate water movement in soils against the experimental data involving a wide range of observed SWCs. The calibration process was carried out for all treatments using collected SWCs in the 2010 growing season. SWC data collected in 2010 one hour before, and immediately and 2, 6, 12, 24, 48, 72, and 96 h after the irrigation events were used in the calibration process. Soil hydraulic properties for the two horizons of the soil profile (i.e., 0–20 cm and 20–80 cm soil depths) were optimized for all treatments using the inverse option of HYDRUS-2D that minimizes deviations between observed and simulated SWCs. During the calibration process, the saturated hydraulic conductivity (K_s), the residual SWC (θ_r), and the saturated SWC (θ_s) were optimized, while parameters α and n were kept equal to values obtained by RETC. HYDRUS-2D was then validated using the calibrated soil hydraulic parameters and daily variations of SWCs during the growing season of 2011.

2.3. Calculation of mass balance components

Once HYDRUS (2D/3D) was calibrated and validated, it was applied to simulate the selected components of the soil water balance for all treatments. The entire rooting zone was first divided into eight rectangular sections 37.5 cm wide and 20 cm deep (i.e., eight sub-regions in HYDRUS (2D/3D) as illustrated in Fig. 3). There were thus four sections on both right and left sides of the rooting zone of a crop. In the PRD treatments, the left side was irrigated during the first week of the stress period while the right side was left to dry out. The irrigated and dry sides were then switched weekly. Both right and left sides were irrigated under the FI and DI treatments.

HYDRUS (2D/3D) directly simulates the temporal variations of all soil water balance components in the rooting zone as well as in the defined sub-regions, including changes in the soil water storage (ΔS), water fluxes (*WF*), and deep percolation (*DP*). Therefore, the actual water uptake (*WU*) from each individual soil layer could be easily calculated by applying soil water balance equation for each soil layer. In addition, HYDRUS (2D/3D) also directly simulates actual soil evaporation (E_a) and actual transpiration (T_a), from which the simulated ET_c was calculated as $ET_c = E_a + T_a$. The daily adjusted crop coefficient ($K_{c,adj}$) was then obtained by dividing daily ET_c by daily reference evapotranspiration (ET_0), which was calculated using the FAO-56 Penman-Monteith equation (Allen et al., 1998) from collected weather data at the experimental site.

In addition to soil water balance components and daily ET_c, the relative available soil water in the soil profile (down to a depth of 80 cm) before each irrigation event was expressed as *BAW* (i.e., Before irrigation relative Available soil Water) and was calculated for all treatments as follows (Nagore et al., 2014):

$$BAW = \frac{\sum_{i=1}^{16}((\theta_{BIi})_T - \theta_{PWPi})}{\sum_{i=1}^{16}(\theta_{FCi} - \theta_{PWPi})} \times 100 \tag{7}$$

where θ_{PWPi} is the SWC at the permanent wilting point of the i^{th} soil layer (i.e., the sum is over 16 soil layers since TRD measurements were taken every 5 cm down to a soil depth of 80 cm).

2.4. Statistical analysis

The root mean square error (*RMSE*), the mean bias error (*MBE*), and the model efficiency (*EF*) were calculated to provide a quantitative assessment of the correspondence between predicted and observed data as follows:

$$RMSE = \sqrt{\frac{\sum_{i=1}^{n}(O_i - P_i)^2}{n}} \tag{8}$$

$$MBE = \frac{\sum_{i=1}^{n}(O_i - P_i)}{n} \tag{9}$$

$$EF = 1 - \frac{\sum_{i=1}^{n}(O_i - P_i)^2}{\sum_{i=1}^{n}(O_i - \overline{O_i})^2} \tag{10}$$

where P_i and O_i are the predicted and observed data, respectively, and n is the number of observations. Collected data was subjected to the analysis of variance (ANOVA) (SAS Institute Inc., 2004), and the standard errors of means (*SEM*) were calculated. The DUNCAN test was applied to compare measured plant variables for plants that were exposed to different irrigation treatments.

3. Results and discussion

3.1. Growth parameters

The leaf area index is a driving factor for crop evapotranspiration and is highly influenced by the water stress (Nagore et al., 2014; Yazar et al., 2009; Howell et al., 2004; Traore et al., 2000). Temporal variations of the leaf area index (LAI) are illustrated in Fig. 4. In the FI treatment, *LAI* increased after the first observation (55 and 40 DAP in 2010 and 2011, respectively) and reached its maximum value 76 DAP in 2010 (4.4 m^2 m^{-2}) and 70 DAP in 2011 (3.6 m^2 m^{-2}). Thereafter, *LAI* declined with time due to crop canopy senescence. *LAI* could be fitted using the second-degree polynomial function except for the DI_{55} treatment in 2011, for which a third-degree polynomial function was fitted (Fig. 4).

Similar to earlier findings (Nagore et al., 2014; Yazar et al., 2009; Howell et al., 2004; Traore et al., 2000), *LAI* was affected by the water stress, except in the PRD_{75} treatment. Compared with the FI treatment, a significant reduction in *LAI* of 5.5%–35% was observed under PRD_{55}, DI_{75}, and DI_{55} treatments. Nevertheless, at all sampling dates, there was no significant difference in *LAI* between the FI and PRD_{75} treatments. Moreover, PRD_{75} led to a 4–25% increase in *LAI* compared to the DI_{75} treatment despite receiving the same amount of irrigation water. This result was also confirmed by Liu et al. (2006).

The root dry mass (*RDM*) is an additional important factor that affects root water uptake. In 2011, *RDM* measured at harvest was 14.8, 17.2, 8.3, 7.6, and 6.1 g plant^{-1} for the FI, PRD_{75}, PRD_{55}, DI_{75}, and DI_{55} treatments, respectively, which is in agreement with the findings of Hu et al. (2009), who reported the root dry mass at harvest to be between 9 and 11 g plant^{-1}. *RDM* for the FI treatment was significantly higher than for the water-saving irrigation treatments, except for the PRD_{75} treatment, for which *RDM* was about

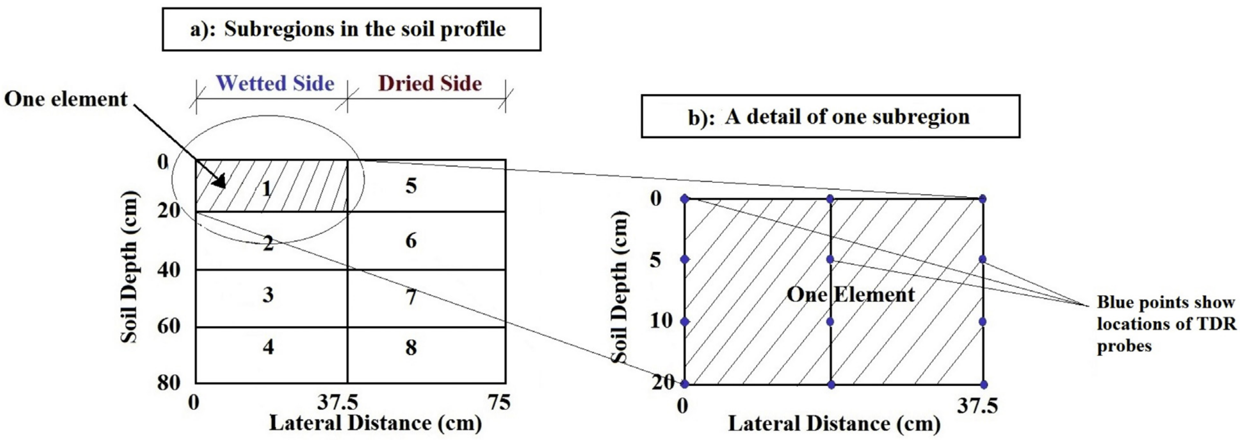

Fig. 3. Sub-regions defined in the transport domain for evaluating soil water balance components by HYDRUS (2D/3D) (a) and a detail of one sub-region (b).

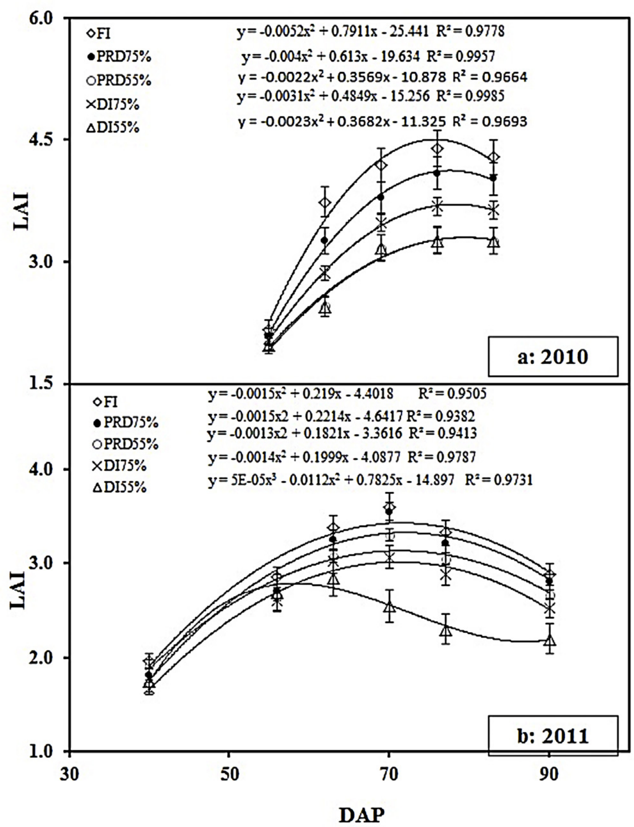

Fig. 4. Time variations of *LAI* for different irrigation treatments (FI, PRD_{75}, PRD_{55}, DI_{75}, and DI_{55}) in 2010 (a) and 2011 (b). Bars indicate the range of *LAI* variations.

16.2% higher than for the FI treatment (significant at $p = 0.05$), and 2.1, 2.3, and 2.8 times higher than for the PRD_{55}, DI_{75}, and DI_{55} treatments, respectively. Alternate wetting and drying of the root system has been reported to have positive effects on root growth under PRD (Liu et al., 2006; Sepaskhah and Ahmadi, 2010; Wang et al., 2012).

3.2. Model efficiency

Based on the model calibration results, optimized parameters θ_s, θ_r, and K_s in FI treatment were 0.47 $cm^3 cm^{-3}$, 0.1 $cm^3 cm^{-3}$, and 1.3 cm day^{-1}, respectively, for the 0–20 cm soil depth and 0.47 $cm^3 cm^{-3}$, 0.071 $cm^3 cm^{-3}$, and 1 cm day^{-1}, respectively, for the 20–80 cm soil depth. Optimized θ_s, θ_r, and K_s for the other treatments are summarized in Table 2. The agreement between observed and simulated SWCs (expressed as equivalent water depths) during the calibration period was quantitatively assessed using the RMSE and MBE statistics (Table 3). The RMSE values ranged from 2.3 to 5.11 mm, indicating a good agreement between the simulated and measured SWCs. Kandelous and Šimůnek (2010) and Wang et al. (2014) reported similar RMSE values of 5–10 mm in their studies. Lower deviations between measured and modeled SWCs were observed for the deeper soil layer, which could probably be attributed to lower changes in the SWCs at greater depths during the calibration process. This is further confirmed by higher deviations near the drippers, where SWC variations were higher. Similar results were reported by Ramos et al. (2012) and Wang et al. (2014). Differences between observed and simulated soil water contents could be a consequence of comparing local simulated soil water contents with measured values that are averaged over a certain soil volume, in which, due to irrigation, the gradient of soil water contents may not be linear and can be quite high, especially around the emission point (Mguidiche et al., 2015).

Fig. 5 compares the temporal variations of the simulated and observed SWCs (averaged over the soil profile) for various irrigation treatments during the cropping cycles of 2010 (the calibration dataset) and 2011 (the validation dataset), to illustrate the capability of HYDRUS-2D in capturing the temporal and spatial trends of *SWCs*. Generally, simulated *SWCs* agreed well with the observed values, with *EF* ranging from 0.893 to 0.998. The close match between simulated and observed SWCs, as well as their seasonal trends, was also obtained in other studies for various soils and crops under pressurized irrigation conditions (Pang et al., 2000; Skaggs et al., 2004; Kandelous and Šimůnek, 2010; Mguidiche et al., 2015).

Comparisons between simulated and measured values of *SWCs* with the 1:1 line in Fig. 5 indicate that HYDRUS-2D can be successfully used to predict daily variations of various components of the soil water balance for both deficit irrigation and partial root-zone drying strategies, as well as for full irrigation. These results indicate that numerical models can be used to develop water-saving irrigation strategies by proposing both optimal irrigation scheduling and an optimal reduction of irrigation water without dramatically decreasing crop yield. The high accuracy of HYDRUS-2D is mainly due to the use of a deterministic approach for simulating soil water movement based on the Richards equation (Doltra and Munoz, 2010). Earlier research has also demonstrated the high potential of HYDRUS-2D for simulating soil water contents under full and deficit irrigation conditions (Cote et al., 2003; Ajdary et al., 2007; Rahil,

Table 2
The optimized parameters θ_s, θ_r, and K_s for different treatments.

θ_r (cm^3 cm^{-3})	θ_s (cm^3 cm^{-3})	K_s (cm day^{-1})	Soil depth (cm)	Treatment
0.10	0.47	1.3	0–20	FI
0.07	0.47	1.0	20–80	
0.10	0.47	1.22	0–20	PRD_{75}
0.08	0.47	0.95	20–80	
0.09	0.47	1.15	0–20	PRD_{55}
0.07	0.47	0.90	20–80	
0.09	0.47	1.10	0–20	DI_{75}
0.10	0.47	0.88	20–80	
0.10	0.47	1.19	0–20	DI_{55}
0.08	0.47	0.93	20–80	

Table 3
Model performance criteria at different soil verticals for the calibration dataset.

Parameter	Time (h)[b]	Position[a]									
		A		B		C		D		E	
		MBE	RMSE[c]	MBE	RMSE	MBE	RMSE	MBE	RMSE	MBE	RMSE
Soil water content in the wetting front	BFI	4.54	4.69	4.54	4.69	4.55	4.70	1.63	2.49	1.95	2.42
	JAI1	−3.05	4.03	−3.50	3.61	2.29	2.36	1.93	2.52	−3.05	4.03
	2 h	4.93	5.11	−3.53	3.64	2.29	2.36	2.35	2.43	−2.47	2.55
	6 h	4.87	5.03	−3.53	3.64	2.28	2.35	2.35	2.43	4.27	4.95
	12 h	4.80	4.96	−3.51	3.62	2.26	2.33	2.34	2.41	−3.60	3.72
	24 h	−3.52	3.63	−3.46	3.57	2.24	2.31	2.31	2.38	−3.52	3.63
	48 h	−3.42	3.52	−3.37	3.47	−1.82	2.44	2.25	2.32	−3.42	3.52
	JAI2	3.00	4.08	−3.45	3.66	2.34	2.41	1.98	2.57	−3.00	4.08
	72 h	3.49	3.66	−3.43	3.60	2.27	2.34	2.34	2.41	−3.49	3.66
	96 h	3.44	3.50	−3.39	3.45	1.84	2.42	2.23	2.30	−3.44	3.50

[a] A: below the first dripper (Fig. 2), B, C, D and E are 18.75, 37.5, 56.25, and 75 cm away from the first dripper, respectively.
[b] BFI – before irrigation; JAI1 – immediately after the first irrigation; 2, 6, 12, 24, 48, 72, and 96 h after the first irrigation, and JAI2–immediately after the second irrigation.
[c] RMSE is the root mean square error and MBE is the mean bias error. Units for both RMSE and MBE are "mm".

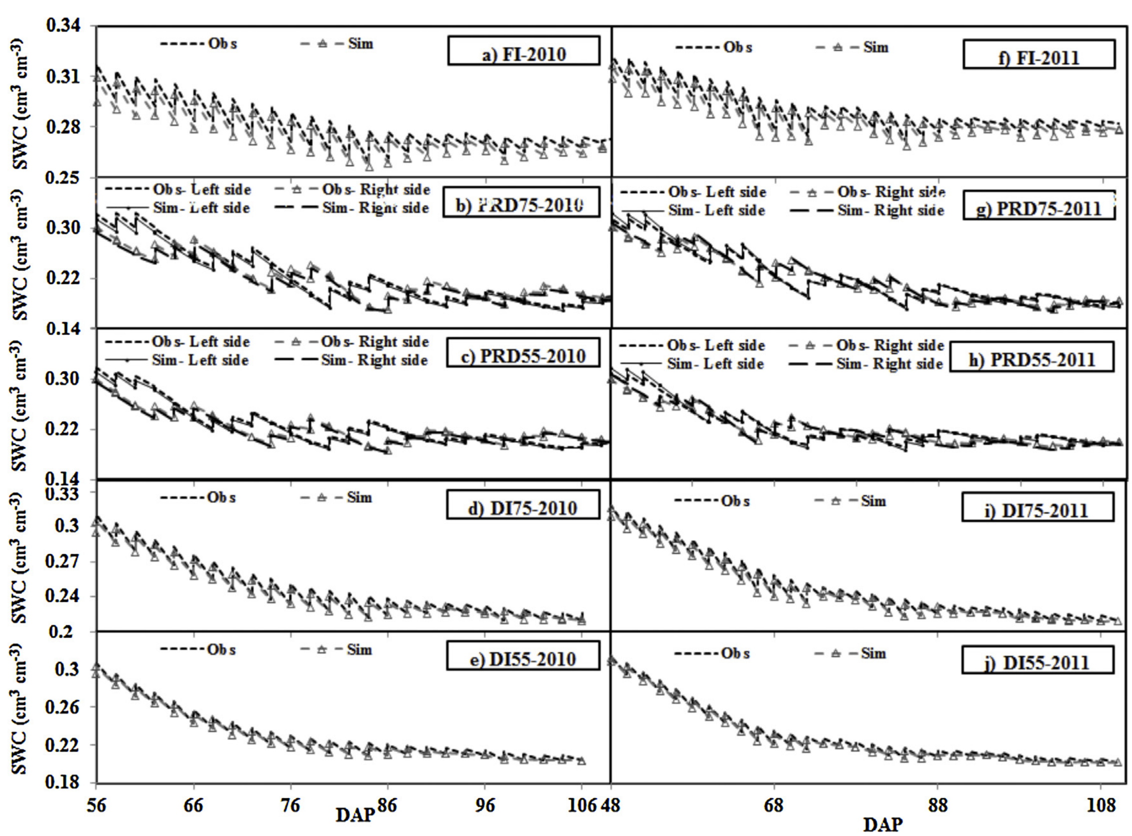

Fig. 5. Observed and simulated *SWCs* during the 2010 (a through e; the calibration dataset) and 2011 (f through j; the validation dataset) growing seasons for different irrigation treatments (FI (a,f), PRD_{75} (b,g), PRD_{55} (c,h), DI_{75} (d,i), and DI_{55} (e,j)).

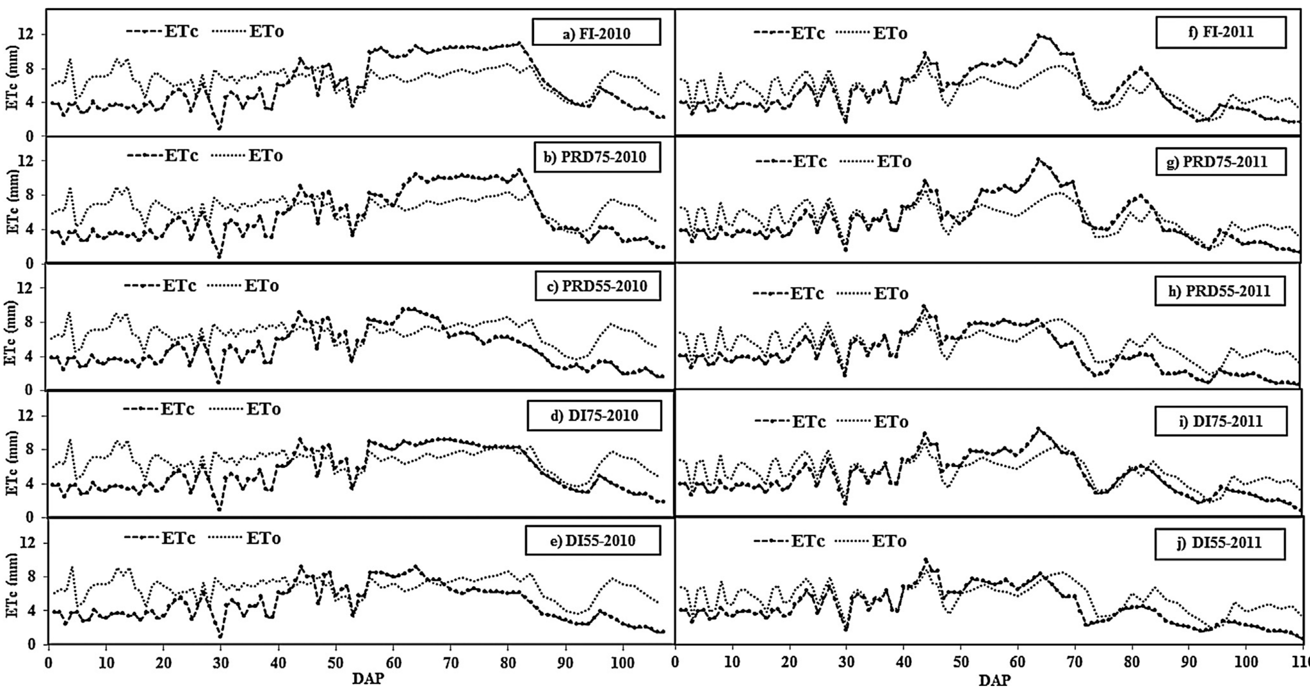

Fig. 6. Temporal variation of ET_0 and simulated ET_c during the 2010 (a through e) and 2011 (f through j) growing seasons for different irrigation treatments (FI (a,f), PRD_{75} (b,g), PRD_{55} (c,h), DI_{75} (d,i), and DI_{55} (e,j)).

2007; Crevoisier et al., 2008; Siyal and Skaggs, 2009; Mubarak, 2009; Tafteh and Sepaskhah, 2012).

3.3. Temporal soil-water-plant interactions

The calibrated and validated HYDRUS-2D model was employed to assess temporal effects of the water stress on soil-water-plant interactions on a daily basis. Daily crop evapotranspiration (ET_c) was simulated for all treatments, and then the daily adjusted crop coefficient ($K_{c,adj}$) was calculated by dividing daily ET_c by daily reference evapotranspiration (ET_0). In addition to ET_c, different components of the soil water balance, *BAW*, and the relative contributions of different soil layers to total root water uptake were also calculated on a daily basis. As discussed below, these simulated results were then used for the analysis of the effects of the water stress on ET_c.

3.3.1. ET_0 and ET_C

ET_0 varied between 2.2 and 9.2 mm d^{-1}, with a mean value of 6.7 mm d^{-1} and a cumulative value of 543.4 mm in the 2010 growing season; it varied between 1.7 and 8.8 mm d^{-1}, with a mean value of 5.5 mm d^{-1} and a cumulative value of 433.6 mm in the 2011 growing season (Fig. 6). Mean daily ET_0 during the maize early-season (before 22 DAP), during the developing stage (23–44 DAP), mid-season (45–82 DAP), and late-season (83–110 DAP) in 2010 were 6.58, 6.85, 7.28, and 5.28 mm d^{-1}, respectively; they were 5.5, 5.9, 6.1, and 4 mm d^{-1}, respectively, in 2011 (Table 4). In agreement with a lower R_n, *VPD*, and *T* (Fig. 1), ET_0 was on average reduced by 20% in 2011 compared to 2010, except during the late season when mean daily ET_0 was about 45% lower than in 2010.

In the FI treatment, the early-season values of ET_c were about 3–4.5 mm d^{-1} and thereafter gradually increased (Fig. 6) to about 8–10 mm d^{-1} in the mid-season, with a few atypical values of 12 mm d^{-1} (Fig. 6). ET_c values then gradually decreased toward the end of the growing season to about 2 mm d^{-1} at harvest. In agreement with ET_0, mean daily ET_c values during the mid- and late-season stages in 2010 were higher than in 2011 in the FI treatment (Table 4). The relatively high ET_c values during these growth stages in 2010 are related to higher climatic parameters, especially higher R_n (Alberto et al., 2014) since climatic conditions are the most dominant factors for ET_c during the mid- and late-season growth stages (Singh and Bhakar, 2002). On the one hand, a larger intercepted R_n in 2010 produced higher *LAI* than in 2011. On the other hand, higher *LAI* produced increased ET_c in 2010 since ET_c was linearly related to *LAI* with R^2 = 0.55–0.92 among different treatments (data not shown). In addition, Fig. 6 shows that despite lower ET_0 in 2011, an increase of about 3.5% and 13.3% in ET_c occurred under the FI treatment during the initial and developing stages, respectively, which is due to the fact that ET_c is more influenced by different irrigation strategies during the vegetation growth stage than by climatic variables (Allen et al., 1998; Shahrokhnia and Sepaskhah, 2013).

Except for the PRD_{75} treatment, the comparative analysis well reflects the negative effect of the water stress on ET_c (Fig. 6 and Table 4). During the stress period, a significant reduction occurred in ET_c and $K_{C,adj}$ under deficit irrigation, which could be associated with a significant reduction in *RDM*. North and Nobel (1991) stated that root growth into the dry soil under deficit irrigation may produce various anatomical changes in the roots, such as the suberization of the epidermis, the collapse of the cortex, and the loss of succulent secondary roots. However, a significantly higher reduction in ET_c during the mid-season stage than during the late-season stage indicated the importance of the plant growth stage in adapting to water stress (Table 4).

Unexpectedly, the PRD_{55} treatment also did not lead to better results compared to the DI_{55} treatment, which may imply that water supplied at a rate of 55% of the evaporative demand could not maintain a high ET_c level, which is in agreement with results reported by Liu et al. (2006). In contrast, compared with the FI treatment, the PRD_{75} treatment led to no significant reduction in ET_c during the water stress period and also resulted in higher ET_c than the other water stress treatments (Fig. 6 and Table 4). The only exception was a one-week period after the onset of the irrigation treatments (55–62 DAP in 2010 and 45–52 DAP in 2011) during

Table 4
ET_o, ET_c, and adjusted K_c for different irrigation treatments (FI, PRD_{75}, PRD_{55}, DI_{75}, and DI_{55}) and different growth stages of maize in 2010 and 2011.

Growth stage	Average K_{Cadj} [a]													
	DAP [b]	FAO [c] 2010	FI	PRD_{75}	PRD_{55}	DI_{75}	DI_{55}	DAP	FAO 2011	FI	PRD_{75}	PRD_{55}	DI_{75}	DI_{55}
Initial stage (K_{cin})	0–22	0.65	0.52	0.52	0.52	0.52	0.52	0–22	0.72	0.66	0.66	0.66	0.66	0.66
Development stage	23–44		0.71	0.71	0.71	0.71	0.71	23–44		0.93	0.93	0.93	0.93	0.93
Mid season stage (K_{cmid})	45–82	1.2	1.26	1.24	1.01	1.13	0.99	45–82	1.2	1.24	1.22	0.91	1.07	0.91
Late season stage	83–107		0.79	0.69	0.49	0.65	0.49	83–110		0.74	0.72	0.50	0.66	0.52
Harvest time (K_{cend})		0.35–0.6	0.45	0.41	0.33	0.38	0.30	–	0.35–0.6	0.54	0.42	0.17	0.25	0.18

Growth stage	Average ET_c (mm d^{-1})													
	DAP	ET_o 2010	FI	PRD_{75}	PRD_{55}	DI_{75}	DI_{55}	DAP	ET_o 2011	FI	PRD_{75}	PRD_{55}	DI_{75}	DI_{55}
Initial stage	0–22	6.85	3.58	3.58	3.58	3.58	3.58	0–22	5.6	3.70	3.70	3.70	3.70	3.70
Development stage	23–44	6.85	4.85	4.85	4.85	4.85	4.85	23–44	5.9	5.50	5.50	5.50	5.50	5.50
Mid season stage	45–82	7.28	9.20	9.00	7.34	8.25	7.23	45–82	6.1	7.55	7.45	5.57	6.50	5.54
Late season stage	83–107	5.82	4.61	3.99	2.86	3.77	2.85	83–110	4.0	2.97	2.90	2.01	2.64	2.08

[a] ET_o = Reference evapotranspiration; Average ET_c = average daily actual evapotranspiration during the considered growth stage; average K_{cadj} = average adjusted crop coefficient during the considered growth stage.
[b] DAP = days after planting.
[c] Recommended K_c for different maize growth stages in FAO-56 (by Allen et al., 1998).

which ET_c under the PRD_{75} treatment was slightly lower than under the DI_{75} treatment on some days. Thereafter, ET_c rapidly increased and exceeded ET_c values for the DI_{75} treatment by about 10–50%. Similarly, Liu et al. (2006) reported lower ET_c under the PRD treatment than under the DI treatment during the 1st day after the onset of the irrigation treatment, which may be associated with reduced soil evaporation under the PRD treatments due to only wetting half of the soil surface during each irrigation event.

The possible causes of PRD_{75}'s ability to maintain ET_c at a favorable level may lie in two major reasons: better utilization of soil water supply and higher *LAI*. Significantly higher *LAI* for PRD_{75} (Fig. 4) led to greater ET_c, which is in agreement with previous studies (NeSmith and Ritchie, 1992; Traore et al., 2000; Howell et al., 2004; Yazar et al., 2009; Nagore et al., 2014). Nevertheless, higher *LAI* in the PRD_{75} treatment could be considered a consequence of better utilization of soil water supply, which will be discussed in Section 3.4.

3.3.2. Adjusted K_C

Fig. 7 shows daily changes in the adjusted crop coefficient ($K_{C,adj}$) for the "stress period" in 2010 and 2011. After the initial stage, $K_{C,adj}$ increased rapidly and reached its maximum value during the mid-season stage. Thereafter, $K_{C,adj}$ decreased toward the late-season stage due to the senescence of maize leaves and reached its minimum value at harvest. The calculated mean $K_{C,adj}$ for different maize growth stages are summarized in Table 4, which also includes the predicted FAO-56 values for K_C for different growth stages.

According to Allen et al. (1998), the adjusted crop coefficient $K_{C,adj}$ is equal to $K_C \times R_S$, where R_S is the stress factor, which is equal to 1 for no-stress conditions and smaller than one for stress conditions. Since irrigation was applied without causing the water stress under the FI treatment ($R_S = 1$), $K_{C,adj}$ is equal to K_C during all growth stages for this treatment. Results showed larger deviations in K_C during different growth stages for well-watered maize under FI than predicted by the FAO values (Table 4). Several reasons may explain the lower $K_{C,ini}$ for the FI treatment (0.52 and 0.66 in 2010 and 2011, respectively) than predicted by FAO-56 (0.65 and 0.72 in 2010 and 2011, respectively). During the initial and development periods, $K_{C,ini}$ is a function of the irrigation interval and the potential evaporation rate and is highly influenced by different irrigation strategies (Allen et al., 1998; Shahrokhnia and Sepaskhah, 2013). Thus, the field management adapted in this study may not be the same as, or even similar to, the normal FAO-56 management. The obtained results are in agreement with studies of Gao et al. (2009) and Mirzaei et al. (2011), who reported that the FAO-predicted K_C values may not always be close to the observed values and poorly predict evaporation during the initial growth stage.

Higher values of $K_{C,mid}$ for the FI treatment than the FAO-predicted values are also supported by the literature: $K_{C,mid}$ = 1.2–1.65 in Liu and Luo (2010); $K_{C,mid}$ = 1.34 in Zhao and Nan (2007); $K_{C,mid}$ = 1.38 in Liu et al. (2002); $K_{C,mid}$ = 1.43 in Kang et al. (2003); and $K_{C,mid}$ = 1.26 in Li et al. (2003). The $K_{C,mid}$ value is less affected by the wetting frequency because vegetation during this stage provides a nearly full ground cover and, the effect of surface evaporation on $K_{C,mid}$ is thus smaller (Singh and Bhakar, 2002). In addition to climate conditions, the crop density and LAI also play a major role in $K_{C,mid}$, which is not directly considered by the FAO-proposed procedure, and that may lead to some deviation in $K_{C,mid}$. On the other hand, $K_{C,end}$ for the FI treatment is in agreement with the FAO-predicted value for $K_{C,end}$.

Similar to ET_c, the comparative analysis revealed no significant differences between FI and PRD_{75} in terms of $K_{C,adj}$ during the stress period (Table 4). In contrast, the water stress under the other water-saving treatments caused about 11–36% reduction in $K_{C,mid}$ and 12–61.5% reduction in $K_{C,end}$. Despite receiving the same amount of irrigation water, daily $K_{C,adj}$ for the DI_{75} treatment was considerably smaller than for the PRD_{75} treatment during both the mid- and late-season stages.

3.4. Soil water utilization

In order to assess the effects of different ET_c patterns under different water-saving irrigation treatments on soil water-plant relationships, temporal variations of the relative soil water content before irrigation (*BAW*) for the 0–80 cm soil depth were calculated for all treatments and plotted in Fig. 8. The soil depth of 80 cm was selected because the root system extended to this depth. Lower *BAW*s for irrigation treatments with the water stress (i.e., PRD and DI) compared to the treatment without the water stress (FI) were evident as early as a few days after initiating water-saving irrigation treatments. During the stress period, the mean *BAW* for the PRD_{75}, PRD_{55}, DI_{75}, and DI_{55} treatments was on average 43, 40.5, 24.5, and 35% lower, respectively, than that for the FI treatment. The difference in *BAW* between the FI treatment and the other water-saving treatments gradually increased until 84 DAP for PRD_{75} and until 72

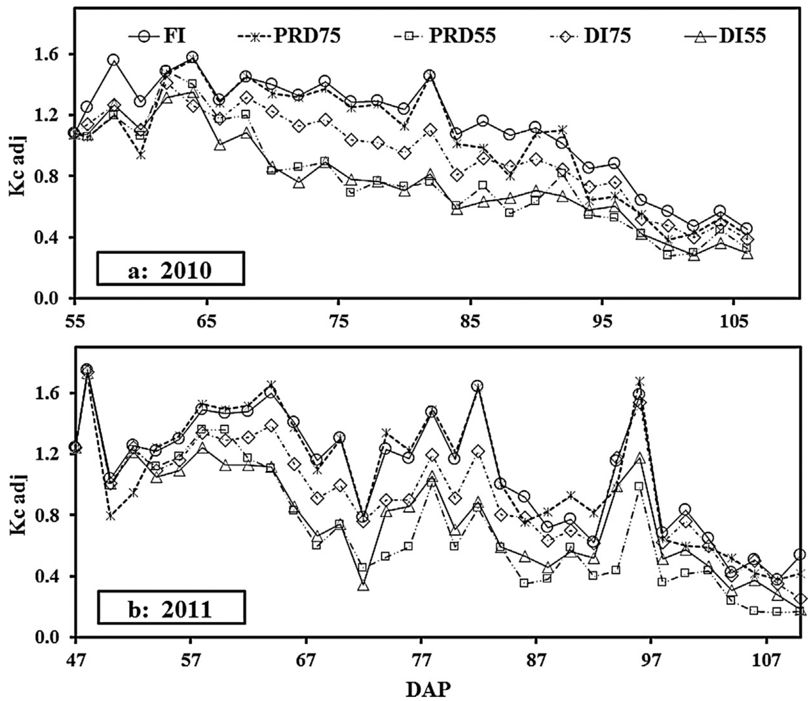

Fig. 7. Daily fluctuations of $K_{C,adj}$ of maize during the "stress period" of 2010 (a) and 2011 (b) for different irrigation treatments (FI, PRD_{75}, PRD_{55}, DI_{75}, and DI_{55}). $K_{C,adj}$ was calculated by dividing simulated ET_c *by* ET_0; ET_0 was calculated using the FAO-56 Penman-Monteith equation.

Table 5
Relative contributions of different soil layers to the total water depletion (*WUi*) in 2010 and 2011 for different irrigation treatments (FI, PRD_{75}, and PRD_{55}). *WU* was calculated based on the results simulated using HYDRUS (2D/3D).

Soil depth (cm)	FI	PRD_{75}	PRD_{55}
WU_i (%) in 2010			
0–20	64.5	51.4	61
20–40	27.2	28.2	26.5
40–60	7.3	17.6	11.8
60–80	1	2.8	0.7
WU_i (%) in 2011			
0–20	63.5	48.6	65
20–40	28.8	22.8	27.5
40–60	6.9	23.4	6.2
60–80	0.8	5.2	1.3

DAP for the other water stress treatments. Thereafter, the differences seemed to be nearly constant until the end of the growing season. Both significantly lower mean *BAW*s and a longer period of gradual reduction of *BAW* under the PRD_{75} treatment compared to the other treatments were evident for both years.

Since a lower *BAW* may be attributed to higher root water uptake, the relative contributions of different soil layers (WU_i) to the total water depletion (*WU*) from 0 to 80 cm soil depths under the FI, PRD_{75}, and PRD_{55} treatments were calculated and summarized in Table 5. A similar water depletion pattern was found for both the FI and PRD_{55} treatments. For the FI treatment, 64, 28, 7.1, and 0.9% of the total water depletion occurred in soil depths of 0–20, 20–40, 40–60, and 60–80 cm, respectively. For the PRD_{55} treatment, the corresponding total water depletion values were 63, 27, 9, and 1%. The water depletion pattern in the PRD_{75} treatment was considerably different than in the other treatments, especially in the soil depths below 40 cm. The contribution of the 40–60 and 60–80 cm soil depths to the total water depletion in the PRD_{75} treatment was 2.8 and 4.4 times higher than in the FI treatment and 2.2 and 4 times higher than in the PRD_{55} treatment, respectively.

A better use of soil water under PRD_{75} is also obvious when the soil water balance components are considered (Table 6). Different irrigation treatments significantly influenced the cumulative evapotranspiration (*cET*) during the stress period. While *cET* in the FI treatment was 400 mm during 55–107 DAP and 370 mm during 45–110 DAP in 2010 and 2011, respectively, *cET* was reduced by 28.8, 14.5, and 30% in the PRD_{55}, DI_{75}, and DI_{55} treatments, respectively, in 2010 and by 27.6, 13.2, and 27.3%, respectively, in 2011. Nevertheless, there was no considerable reduction of *cET* in the PRD_{75} treatment compared to that in the FI treatment. PRD_{75} increased *cET* by 9.6-35.8% compared to other water-saving irrigation treatments during the stress period. Moreover, the water stress, under water-saving treatments, caused an increased use of the initially available soil water (ΔS) compared to the FI treatment in which crops were fully irrigated (Table 6). However, a significantly higher ΔS for PRD_{75} than for the other treatments was obvious in both seasons.

Higher ΔS and lower *BAW* under the PRD_{75} treatments reflect a considerable increase in the soil water extraction capacity (Fig. 8 and Table 6). Such results are confirmed when deep percolation under different treatments is considered. As stated previously, while the irrigation volume at one dripper line was increased by 50 and 10% in the PRD_{75} and PRD_{55} treatments, respectively, the other dripper line was alternatively not used at all. Therefore, higher *DP* can be expected under the PRD_{75} treatment since half of the rooting zone in this treatment receives 50% more irrigation water than the corresponding side under the FI treatment (Table 6). However, simulated water fluxes out of the rooting zone (*DP*) indicate that *DP* ceased under the PRD_{75} treatment after 62 and 52 DAP in 2010 and 2011, respectively. This result demonstrated that the soil water content at the wetted side of the row of PRD plants is depleted more rapidly than at the same side of control (FI) plants, indicating that the root system can partially compensate for the increasingly limited water availability at the dry side of the row (Kang et al., 2003).

The better utilization of the soil water content could be ascribed to a significant increase in the root dry mass (*RDM*) under the PRD_{75}

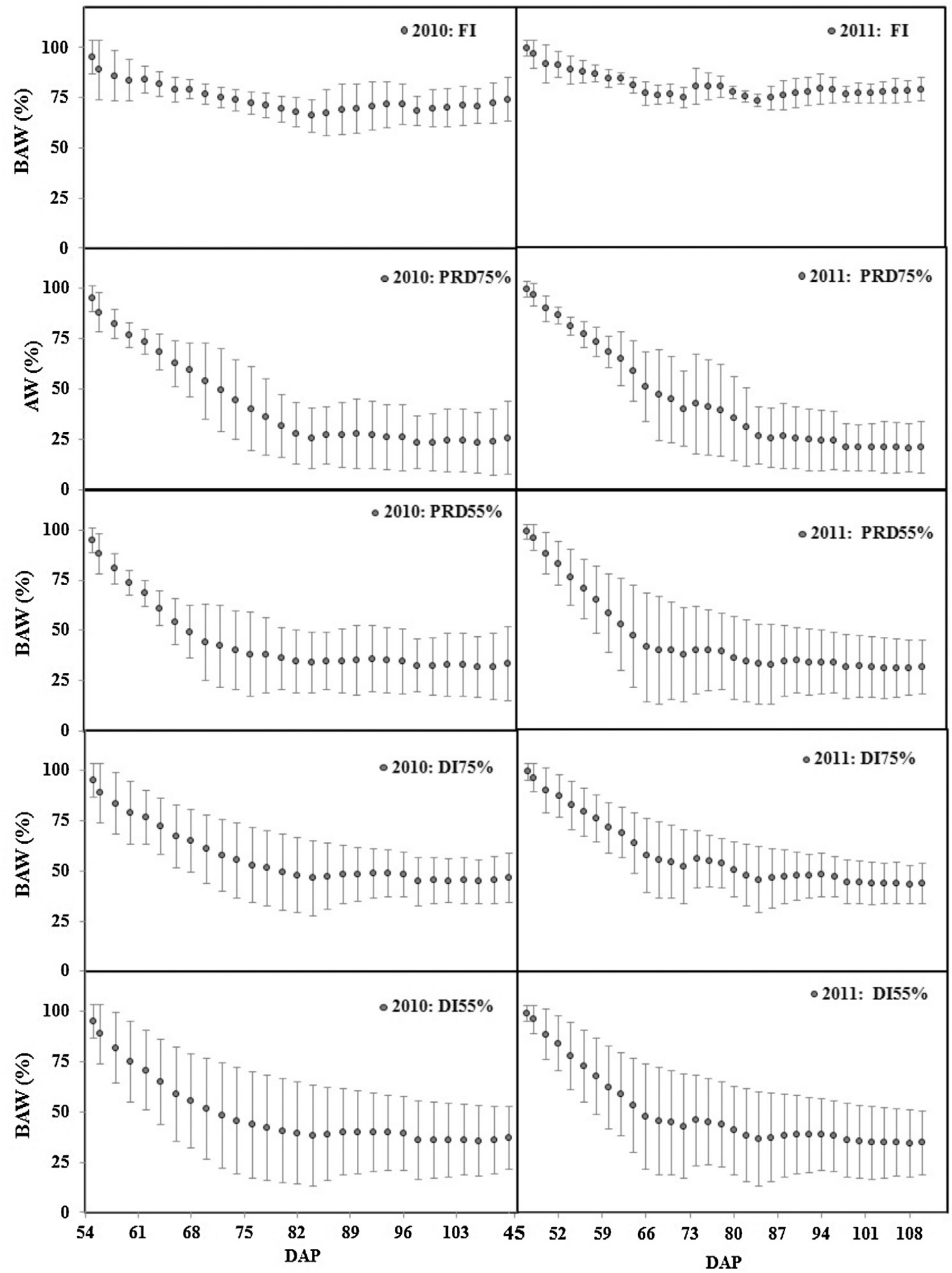

Fig. 8. Temporal variations of *BAW* of the 0–80 cm soil depth during the stress period of 2010 (left) and 2011 (right) for different irrigation treatments (FI, PRD_{75}, PRD_{55}, DI_{75}, and DI_{55}). Bars indicate variations of calculated *BAW* (using Eq. (10)) for all measured points in the 0–80 cm soil depth.

treatment. More root biomass could also be associated with a significant increase in the root density. A higher contribution from a deeper soil layer (40–80 cm) to the total water depletion in the PRD_{75} treatment than in the other treatment (Table 5) also confirmed a notable increase in the root density in deeper soil layers. A higher root density may imply that the root surface area of the PRD_{75} plants was also higher (Wang et al., 2012). The root surface area has been reported to have a big effect on water and nutrient uptake from the soil matrix (Wang et al., 2012). Thus, it is plausible to state that a significantly higher *RDM* in the PRD_{75} treatment caused a significant increase in the soil water extraction capacity and a better utilization of soil water supply.

A higher water extraction capacity due to higher *RDM* under PRD_{75} is in agreement with the findings of other studies. Sepaskhah and Ahmadi (2010) reported that the root system can partially compensate for decreasing water availability on the non-irrigated side of PRD due to an increase in the root hydraulic conductivity. Liu et al. (2006) reported that more soil water depletion occurred under PRD than under other deficit irrigation strategies due to a higher root hydraulic conductivity. Thus, significantly higher *RDM* and root density at deeper soil layers improved the ability of the PRD_{75} plants to absorb more water from the soil matrix (Liang et al., 1996). In addition to the positive effect of increased *RDM* on an increase in the soil water extraction capacity and consequently ET_c, higher ET_c under PRD_{75}, despite a lower mean *BAW* during the stress period, may indicate a lower available soil water threshold, below which actual *ET* in the other water-saving treatments is reduced with respect to its maximum value in the PRD_{75} treatment. Nagore et al. (2014) also reported a lower water content threshold for the *ET* reduction for a new maize hybrid than in the older ones.

Table 6
Soil water balance components for different irrigation treatments (FI, PRD_{75}, PRD_{55}, DI_{75}, and DI_{55}) in 2010 and 2011. *cET*, *DP*, and ΔS were simulated using HYDRUS (2D/3D) while *I* and *P* were directly measured in the field.

Water balance components*	*I* (mm)	*cET* (mm)	*P* (mm)	*DP* (mm)	ΔS (mm)	*I* (mm)	*cET* (mm)	*P* (mm)	*DP* (mm)	ΔS (mm)
Treatments	2010 (during the stress period)***						2010 (during the entire growing season)			
FI	372	400^{a}**	0	0	28	613	649	8	0	28^{d}
PRD_{75}	279	375^{ab}	0	13.3	109	520	624	8	13.3	109.3^{a}
PRD_{55}	204	285^{c}	0	0	81	445	534	8	0	81b
DI_{75}	279	342^{b}	0	0	63	520	591	8	0	63^{c}
DI_{55}	204	280^{c}	0	0	76	445	529	8	0	76^{b}
	2011 (during the stress period)						2011 (during the entire growing season)			
FI	361	370^{a}	0	0	9.6	523	572	40	0	9.6
PRD_{75}	271	364^{a}	0	11	104	433	566	40	11	104
PRD_{55}	199	268^{c}	0	1	70	361	470	40	1	70
DI_{75}	271	321^{b}	0	0	50	433	523	40	0	50
DI_{55}	199	269^{c}	0	0	70	361	471	40	0	70

* Soil water balance components include irrigation (*I*), cumulative evapotranspiration (*cET*), precipitation (*P*), deep percolation (*DP*) and a change in soil water storage (ΔS); ΔS ($\Delta S = S_1 - S_2$) was calculated as a difference between the soil water content at the beginning (S_1) and the end of a specific time period (S_2). *I* and *P* were measured, while ET_c, *DP*, and ΔS were obtained by HYDRUS (2D/3D).
** Same letters indicate no significant differences between treatments ($p < 0.05$).
*** The stress period was during 55–107 DAP in 2010 and during 45–110 DAP in 2011 when different irrigation treatments were applied. Before the start of the stress period, all treatments received the same amount of irrigation water in all irrigation events (before 55 DAP in 2010 and 45 DAP in 2011).

Table 7
Maize grain yields (Y) for different irrigation treatments (FI, PRD_{75}, PRD_{55}, DI_{75}, and DI_{55}) in 2010 and 2011.

Treatment	*Y* (Mg ha^{-1}) 2010	2011
FI	7^{a}*	6.6^{a}
PRD_{75}	6.9^{a}	6.2^{a}
DI_{75}	5.8^{b}	5.3^{b}
PRD_{55}	3.3^{c}	5.7^{ab}
DI_{55}	3.2^{c}	4.9^{c}

* Same letters indicate no significant difference between treatments ($p < 0.05$).

3.5. Maize grain yield

The grain yield (*Y*) was significantly affected by different irrigation treatments. The grain yield for the FI, PRD_{75}, PRD_{55}, DI_{75}, and DI_{55} treatments was 7, 6.9, 3.3, 5.8, and 3.2 t ha^{-1}, respectively, in 2010, and 6.6, 6.2, 5.7, 5.3, and 4.9 t ha^{-1}, respectively, in 2011 (Table 7). The statistical analysis revealed that the water stress led to a significant reduction in *Y* for the PRD_{55}, DI_{75}, and DI_{55} treatments compared to the FI treatment, while it caused no significant reduction in *Y* for the PRD_{75} treatment. Higher ET_c and $K_{C,adj}$, due to a better utilization of soil water supply and consequently, higher *LAI*, caused PRD_{75} to produce a significantly higher grain yield than the other water-saving treatments; there was no significant difference between *Y* in the FI and PRD_{75} treatments. Regardless of the growing season, a relative grain yield (Y_a/Y_m where Y_a is the actual grain yield, and Y_m is the maximum grain yield) was closely associated with relative seasonal *ET* (ET_a/ET_m where ET_a and ET_m are the actual and maximum *ET*, respectively) in different treatments ($R^2 = 0.70$ and 0.86 for 2010 and 2011, respectively). The positive effect of favorable ET_c on maintaining the maize grain yield has also been reported by other researchers (Stone, 2003; Klocke et al., 2004).

4. Conclusions

A global water crisis and increased population growth necessitate special attention to water consumption management in the agricultural sector. Water-saving irrigation strategies are assured solutions under the conditions of water scarcity, while their effects on food security still needs to be assessed. Combined field and model investigations were thus carried out in a drip-irrigated maize field to evaluate the influence of water stress on soil-water-plant interactions under deficit irrigation (DI) and partial root-zone drying (PRD). The quantitative analysis indicated the capability of the HYDRUS-2D model to simulate both values and temporal-trends of soil water balance components. Simulated results and field data reflected well the significant influence of the irrigation water management on water-yield functions. The special soil water status under the PRD_{75} treatment improved root repartitions, resulting in a better utilization of soil water supply through enhanced water uptake from deeper soil layers. As a result, actual crop evapotranspiration was maintained at a favorable level and no significant yield loss was observed under PRD_{75}. In fact, optimal management under PRD_{75} led to a considerable increase in the water use efficiency despite receiving 25% less irrigation water compared to full irrigation. These concluding remarks are further confirmed when the negative results under DI with the same reduction in the irrigation water depth as that for PRD_{75} are considered. PRD_{75} is thus the most efficient water-saving irrigation strategy for maize cultivation in the study area. Additionally, it could be concluded that the HYDRUS-2D model, instead of labor- and time-consuming and expensive field investigations, could be reliably used for determining the optimal soil-water-plant interactions under both DI and PRD strategies.

References

Ajdary, K., Singh, D.K., Singh, A.K., Khanna, M., 2007. Modeling of nitrogen leaching from experimental onion field under drip fertigation. Agric. Water Manage. 89, 15–28.
Alberto, M.C.R., Quilty, J.R., Buresh, R.J., Wassmann, R., Haidar, S., Correajr, T.Q., Sndro, J.M., 2014. Actual evapotranspiration and dual crop coefficient for dry-seeded rice and hybrid maize growth with overhead sprinkler irrigation. Agric. Water Manage. 136, 1–12.
Allen, R.G., Pereira, L.S., Raes, D., Smith, M., 1998. Crop evapotranspiration guide Lines for computing crop water requirements. Irrigation and Drainage Paper 56, FAO, Rome, Italy. p. 300.
Bar-Yosef, B., Sheikholslami, M.R., 1976. Distribution of water and ions in soils irrigated and fertilized from a trickle source. Soil Sci. Soc. Am. J. 40, 575–582.
Belmans, C., Wesseling, J.G., Feddes, R.A., 1983. Simulation model of the water bal-ance of a cropped soil: SWATRE. J. Hydrol. 63 (3), 271–286.
Cote, C.M., Bristow, K.L., Charlesworth, P.B., Cook, F.J., Thorburn, P.J., 2003. Analysis of soil wetting and solute transport in subsurface trickle irrigation. Irrig. Sci. 22, 143–156.
Crevoisier, D., Popova, Z., Mailhol, J.C., Ruelle, P., 2008. Assessment and simulation of water and nitrogen transfer under furrow irrigation. Agric. Water Manage. 95, 354–366.
Darzi-Naftchali, A., Shahnazari, A., 2014. Influence of subsurface drainage on the productivity of poorly drained paddy fields. Europ. J. Agron. (in press).
Doltra, J., Munoz, P., 2010. Simulation of nitrogen leaching from a fertigation crop rotation in a Mediterranean climate using the EU-Rotate-N and HYDRUS-2D models. Agric. Water Manage. 97, 277–285.

Dry, P.R., Loveys, B.R., 1998. Factors influencing grapevine vigor and the potential for control with partial rootzone drying. Aust. J. Grape Wine Res. 4, 140–148.
Dry, P.R., Loveys, B.R., During, H., 2000. Partial drying of the rootzone of grape: 2. Changes in the patterns of root development. Vitis 39, 9–12.
Feddes, R.A., Kowalik, P.J., Zaradny, H., 1978. Simulation of field water use and crop yield. In: Simulation Monographs. Pudoc, Wageningen.
Gärdenäs, A.I., Hopman, J.W., Hanson, B.R., Šimůnek, J., 2005. Two-dimensional modeling of nitrate leahing for various fertigation scenarios under micro-irrigation. Agric. Water Manage. 74 (3), 219–242.
Gao, Y., Duna, A., Sun, J., Li, F., Liu, Z., Liu, H., Liu, Z., 2009. Crop coefficient and water-use efficiency of winter wheat/spring maize strip intercropping. Field Crop Res. 111, 65–73.
Howell, T.A., Evett, S.R., Tolk, J.A., Scheider, A.D., 2004. Evapotranspiration of full-, deficit-irrigated, and dry land cotton on the Northern Texas high plains. J. Irrig. Drain. 130 (4), 277–285.
Hu, T., Kang, S., Li, F., Zhang, J., 2009. Effects of partial root-zone irrigation on thenitrogen absorption and utilization of maize. Agric. Water Manage. 96, 208–214.
Kandelous, M.M., Šimůnek, J., 2010. Numerical simulations of water movement in a subsurface drip irrigation system under field and laboratory conditions using HYDRUS-2D. Agric. Water Manage. 97, 1070–1076.
Kang, S., Zhang, J., 2004. Controlled alternate partial root-zone irrigation: its physiological consequences and impact on water use efficiency. J. Exp. Bot. 55, 2437–2446.
Kang, S., Gu, B., Du, T., Zhang, J., 2003. Crop coefficient and ratio of transpiration to evapotranspiration of winter wheat and maize in a semi-humid region. Agric. Water Manage. 59 (3), 239–254.
Karandish, F., Šimůnek, J., Numerical and machine-learning modeling of soil water content for sustainable water management in agriculture under water stress, Journal of Hydrology, (in review).
Karandish, F., Shahnazari, A., 2016. Soil temperature and maize nitrogen uptake improvement under partial root zone drying. Pedosphere (in press).
Karandish, F., Salari, S., Darzi-Naftchali, A., 2015. Application of virtual water trade to evaluate cropping pattern in arid regions. Water Resour. Manage. 29 (11), 4061–4074, http://dx.doi.org/10.1007/s11269-015-1045-4.
Kirda, C., Cetin, M., Dasgan, Y., Topcu, S., Kaman, H., Ekici, B., Derici, M.R., Ozguven, A.I., 2004. Yield response of greenhouse grown tomato to partial root drying and conventional deficit irrigation. Agric. Water Manage. 69, 191–201.
Klocke, N.L., Schneekloth, J.P., Melvin, S., Clark, R.T., Payero, J.O., 2004. Field scale limited irrigation scenarios for water policy strategies. Appl. Eng. Agric. 20, 623–631.
Kumar, K., Prihar, S.S., Gajri, P.R., 1993. Determination of root distribution of wheat by auger sampling. Plant Soil 149, 245–253.
Li, J., Liu, Y., 2011. Water and nitrate distributions as affected by layered-textural soil and buried dripline depth under subsurface drip fertigation. Irrig. Sci. 29, 469–478.
Li, Y.L., Cui, J.Y., Zhang, T.H., Zhao, H.L., 2003. Measurement of evapotranspiration of irrigated spring wheat and maize in a semi-arid region of north China. Agric. Water Manage. 61 (1), 1–12.
Liang, J., Zhang, J., Wong, M.H., 1996. Effects of air-filled soil porosity and aeration on the initiation and growth of secondary roots of maize (Zea mays). J. Plant Soil 186, 245–254.
Liu, Y.J., Luo, Y., 2010. A consolidated evaluation of the FAO-56 dual crop coefficient approach using the lysimeter data in the North China Plain. Agric. Water Manage. 97, 31–40.
Liu, C., Zhang, X., Zhang, Y., 2002. Determination of daily evaporation and evapotranspiration of winter wheat and maize by large-scale weighing lysimeter and micro-lysimeter. Agric. For. Meteorol. 111, 109–120.
Liu, F., Shahnazari, A., Andersen, M.N., Jacobsen, S.E., Jensen, C.R., 2006. Effects of deficit irrigation (DI) and partial root drying (PRD) on gas exchange biomass partitioning, and water use efficiency in potato. Sci. Hortic. 109, 113–117.
Mguidiche, A., Provenzano, G., Douh, B., Khila, S., Rallo, G., Boujelben, A., 2015. Assessing HYDRUS-2D to simulate soil water content (SWC) and salt accumulation under an SDI system: application to a potato crop in a semi-arid area of central Tunisia. Irrig. Drain. 64, 263–274.
Mirzaei, M., Sohrabi, T., Jahanbania, H., Faghih, M., Teang, S.L., 2011. Evaluation of evapotranspiration coefficient and daily crop reference evapotranspiration in a semi-arid region based on field water balance and FAO method. Aust. J. Basic Appl. Sci. 5 (12), 1850–1856.
Mualem, Y., 1976. A new model for predicting the hydraulic conductivity of unsaturated porous media. Water Resour. Res. 12, 513–522.
Mubarak, I., 2009. Effect of temporal variability in soil hydraulic properties on simulated water transfer under high-frequency drip irrigation. Agric. Water Manage. 96 (11), 1547–1559.
Nagore, M.L., Echarte, L., Andrade, F.H., Maggiora, A.D., 2014. Crop evapotranspiration in Argentina maize hybrids released. Field Crop Res. 155, 23–29.
NeSmith, D.S., Ritchie, J.T., 1992. Effects of soil water deficits during tassel emergence on development and yield component of maize (Zea mays). Field Crops Res. 28, 251–256.
North, G.B., Nobel, P.S., 1991. Changes in hydraulic conductivity and anatomy caused by drying and rewetting roots of Agave-Deserti (Agavaceae). Am. J. Bot. 78, 906–915.
OECD, 2010. Sustainable Management of Water Resources in Agriculture. OECD Publishing, p 120.
Pang, L., Close, M.E., Watt, J.P.C., Vincent, K.W., 2000. Simulation of picloram, atrazine and simazine through two New Zealand soils and into groundwater using HYDRUS-2D. J. Contam. Hydrol. 44, 19–46.
Payero, J.O., Melvin, S.R., Irmak, S., Tarkalson, D., 2006. Yield response of corn to deficit irrigation in a semiarid climate. Agric. Water Manage. 84, 101–112.
Rahil, M.H., 2007. Simulating soil water flow and nitrogen dynamics in a sunflower field irrigated with reclaimed wastewater. Agric. Water Manage. 92 (3), 142–150.
Ramos, T.B., Šimůnek, J., Goncalves, M.C., Martins, J.C., Prazeres, A., Pereira, L.S., 2012. Two-dimensional modeling of water and nitrogen fate from sweet sorghum irrigated with fresh and blended saline waters. Agric. Water Manage. 111, 87–104.
Ritchie, J.T., 1972. Model for predicting evaporation from a row crop with incomplete cover. Water Resour. Res. 8, 1204–1213.
SAS Institute, 2004. Version 9.1.3. SAS Institute, Cary, NC, USA.
Sepaskhah, A.R., Ahmadi, S.H., 2010. A review on partial root-zone drying irrigation. Int. J. Plant Prod. 4 (4), 241–258.
Shahnazari, A., Liu, F., Andersen, M.N., Jacobsen, S.E., Jensen, C.R., 2007. Effects of partial root-zone drying on yield: tuber size and water use efficiency in potato under field conditions. Field Crops Res. 100, 117–124.
Shahrokhnia, M.H., Sepaskhah, A.R., 2013. Single and dual crop coefficient and crop evapotranspiration for wheat and maize in a semi-arid region. Theor. Appl. Climatol. 114, 495–510.
Shao, G.C., Zhang, Z.Y., Liu, N., Yu, S.E., Xing, W.G., 2008. Comparative effects of deficit irrigation (DI) and partial rootzone drying (PRD) on soil water distribution, water use, growth and yield in greenhouse grown hot pepper. Hortic. Sci. 119 (1), 11–16.
Šimůnek, J., van Genuchten, M.Th., Šejna, M., 2008. Development and applications of the HYDRUS and STANMOD software packages and related codes. Vadose Zone J. 7 (2), 587–600, http://dx.doi.org/10.2136/VZJ2007.0077.
Šimůnek, J., van Genuchten, M.Th., Šejna, M., 2011. The HYDRUS Software Package for Simulating Two- and Three-Dimensional Movement of Water, Heat, and Multiple Solutes in Variably-Saturated Media. Technical Manual, Version 2. PC Progress, Prague, Czech Republic, pp. 258.
Šimůnek, J., van Genuchten, M.Th., Šejna, M., 2016. Recent developments and applications of the HYDRUS computer software packages. Vadose Zone J. 15 (7), 25, http://dx.doi.org/10.2136/vzj2016.04.0033.
Singh, R.V., Bhakar, S.R., 2002. Development of improved crop coefficients for precise estimates of wheat evapotranspiration. Asian Agricultural Information Technology and Management. In: Proceedings of the Third Asian Conference for Information Technology in Agriculture, Beijing, China, 26–28 October, pp. 333–337.
Siyal, A.A., Skaggs, T.H., 2009. Measured and simulated soil wetting patterns under porous clay pipe sub-surface irrigation. Agric. Water Manage. 96 (6), 893–904.
Skaggs, T., Trout, T., Šimůnek, J., Shouse, P., 2004. Comparison of HYDRUS-2D simulations of drip irrigation with experimental observations. J. Irrig. Drain. Eng. 130, 304–310.
Stoll, M., Loveys, B., Dry, P., 2000. Improving water use efficiency of irrigated horticultural crops. J. Exp. Bot. 51, 1627–1634.
Stone, L.R., 2003. Crop water use requirements and water use efficiencies. In: Proceedings of the 15th Annual Central Plains Irrigation Conference and Exposition, Colby, Kansas, pp. 127–133.
Tafteh, A., Sepaskhah, A.R., 2012. Application of HYDRUS-1D model for simulating water and nitrate leaching from continuous and alternate furrow irrigated rapeseed and maize fields. Agric. Water Manage. 113, 19–29.
Tang, L.S., Li, Y., Zhang, J., 2005. Physiological and yield responses of cotton under partial root-zone irrigation. Field Crop Res. 94, 214–223.
Traore, S.B., Carlson, R.E., Pilcher, C.D., Rice, M.E., 2000. Bt and Non-Bt maize growth and development as affected by temperature and drought stress. J. Agron. 92, 1027–1035.
van Genuchten, M.T., 1980. A closed-form equation for predicting the hydraulic conductivity of unsaturated soils. Soil Sci. Soc. Am. J. 44, 892–898.
Vrugt, J.A., Hopmans, J.W., Šimůnek, J., 2001. Calibration of a two-dimensional root water uptake model. Soil Sci. Soc. Am. J. 65 (4), 1027–1037.
Wang, Z., Liu, F., Kang, Sh., Jensen, C.R., 2012. Alternate partial root-zone drying irrigation improves nitrogen nutrition in maize (Zea mays L.) leaves. Environ. Exp. Bot. 75, 36–40.
Wang, Z., Li, J., Li, Y., 2014. Simulation of nitrate leaching under varying drip system uniformities and precipitation patterns during the growing season of maize in the North China Plain. Agric. Water Manage. 142, 19–28.
Yazar, A., Gokcel, F., Sezen, M.S., 2009. Corn yield response to partial root-zone drying and deficit irrigation strategies applied with drip system. Plant Soil Environ. 55 (11), 494–503.
Zhao, C., Nan, Z., 2007. Estimating water needs of maize (Zea mays L.) using the dual crop coefficient method in the arid region of northwestern China. Afr. J. Agric. Res. 2 (7), 325–333.